# Modelling the spring ozone maximum and the interhemispheric asymmetry in the remote marine boundary layer
# 1. Comparison with surface and ozonesonde measurements



[1]K.-Y. Wang, [2]D.E. Shallcross, and [3]J.A. Pyle

1. Department of Atmospheric Sciences, National Central University, Chung-Li, Taiwan

2. Centre for Biogeochemistry, School of Chemistry, Bristol University, BS8 1TS, U.K.

3. Centre for Atmospheric Science, Cambridge University, CB2 1EW, U.K.

Short title: MARINE BOUNDARY LAYER OZONE

**Abstract.** Here we report a modelling study of the spring ozone maximum and its interhemispheric asymmetry in the remote marine boundary layer (MBL). The modelled results are examined at the surface and on a series of time-height cross sections at several locations spread over the Atlantic, the Indian, and the Pacific Oceans. Comparison of model with surface measurements at remote MBL stations indicate a close agreement. The most striking feature of the hemispheric spring ozone maximum in the MBL can be most easily identified at the NH sites of Westman Island, Bermuda, and Mauna Loa, and at the SH site of Samoa. Modelled ozone vertical distributions in the troposphere are compared with ozone profiles. For the Atlantic and the Indian sites, the model generally produces a hemispheric spring ozone maximum close to those of the measurements. The model also produces a spring ozone maximum in the northeastern and tropical north Pacific close to those measurements, and at sites in the NH high latitudes. The good agreement between model and measurements indicate that the model can reproduce the proposed mechanisms responsible for producing the spring ozone maximum in these regions of the MBL, lending confidence in the use of the model to investigate MBL ozone chemistry (see part 2 and part 3). The spring ozone maximum in the tropical central south Pacific and eastern equatorial Pacific are less well reproduced by the model, indicating that both the transport of $O_3$ precursors from biomass burning emissions taking place in southeastern Asia, Australia, Oceania, southern Africa, and South America are not well represented in the model in these regions. Overall, the model produces a better simulation at sites where the stratosphere and biomass burning emissions are the major contributors.

*Key word index:* ozone, CTM, spring ozone maximum, interhemispheric asymmetry, biomass burning

## 1. Introduction

Due to its impact on human health [e.g., *Künzli et al.*, 2000] and terrestrial vegetation [e.g., *Finnan et al.*, 1996], and its role as a greenhouse gas, ozone has long been intensively studied via surface and ozonesonde measurements, aircraft observations, satellite total ozone mapping, and numerical modelling. Many long-term and intensive surface ozone measurements in the remote marine environment had been conducted over the Atlantic [e.g., *Winkler*, 1988; *Penkett et al.*, 1998; *Junkermann and Stockwell*, 1999], the Pacific [e.g., *Piotrowicz et al.*, 1986; *Piotrowicz et al.*, 1991; *Jaffe et al.*, 1996; *Crawford et al.*, 1997; *Kajii et al.*, 1997; *Pochanart et al.*, 1999; *Monks et al.*, 2000], and the Indian Ocean [e.g., *Lal et al.*, 1998]. Since there are limitations in observations of ozone and other constituents primarily at the surface, many measurements such as ozonesonde [e.g., *Moody et al.* [1995]; *Oltmans et al.*, 1996; *Logan*, 1999, and references therein; *Latt et al.*, 1999], and airplanes [e.g., *Kawa and Pearson*, 1989; *Murphy and Fahey*, 1994] were used to provide the necessary profile information for understanding the chemistry and dynamics controlling the variations of ozone in the troposphere.

*Monks* [2000] gave a comprehensive review of the surface observations and the springtime ozone maximum, while *Logan* [1999] documented ozonesonde measurements and derived a climatology for tropospheric ozone based on these sonde data. Two prominent features constantly show up from these measurements. First, the appearance of a spring maximum in the troposphere; and secondly, the existence of an interhemispheric asymmetry between the northern and southern hemispheres [e.g.,

*Winkler*, 1988; *Johnson et al.*, 1990]. These interhemispheric asymmetries also featured in three-dimensional (3D) modelling studies [e.g., *Müller and Brasseur*, 1995].

Basically there are two theories regarding the origins of elevated ozone in the remote troposphere. First, transport from the stratosphere to the troposphere is the dominating source of ozone in the troposphere [e.g., *Moody et al.*, 1995; *Oltmans et al.*, 1996; *Roelofs and Lelieveld*, 1997]. Second, that tropospheric ozone originated mainly from emissions (e.g., biomass burning emissions of $O_3$ precursors, and NOx sources from soil and lightning in the continents), photochemistry (photochemical oxidation of CO and hydrocarbons catalysed by HOx and NOx [e.g., see *Monks*, 2000, and references therein]), and transport processes (e.g., large-scale long-range transport, cloud convection, and vertical mixing between the atmospheric boundary layer and free troposphere) within the troposphere [*Roelofs et al.*, 1997; *Yinger et al.*, 1999; *Logan*, 1999]. The general consensus is that the elevated ozone concentrations in the remote MBL are non-indigenous, and the transport of either or both elevated ozone and its precursors from elsewhere is the major contributing factor for the observed high ozone levels in the remote MBL. In addition, very low ozone concentrations have also been observed in the tropical MBL [*Kley et al.*, 1996; *Singh et al.*, 1996], indicating that halogens may play an important role in oxidation processes and the ozone budget in parts of the remote MBL [*Ariya et al.*, 1998; *Dickerson et al.*, 1999; *Nagao et al.*, 1999].

Hence modelling the spring ozone maximum and interhemispheric asymmetry remains one of the most critical tests to our current understanding of tropospheric chemistry in the remote MBL [*Winkler*, 1988; *Logan*, 1999; *Monks*, 2000]. The recently

available ozonesonde measurements provide a much higher global coverage of the ozone vertical profiles from surface to the lower stratosphere; however, these ozonesondes have not yet been widely used to address the issue such as spring ozone maximum and interhemispheric asymmetry [e.g., *Logan*, 1999]. In this first part of a three-part series of papers, concerning the sources of the spring ozone maximum and its interhemispheric asymmetry in the remote MBL, we present results from a 3D chemistry transport model (CTM) and a detailed annual comparison with surface and ozonesonde measurements at several locations in the remote marine environments. A modelling test on the *stratosphere-dominated theory* is discussed in the second part of the paper. Finally, the test on the *self-contained theory* is discussed in the final part of the paper.

## 2. The IMS Model

A detailed description about the formulation and evaluation of model emission inventories, transport processes, chemistry, and the simulated $O_3$, $CH_4$, and CO distributions in the troposphere were described in *Wang et al.* [2001], *Wang et al.* [1999], and *Wang and Shallcross* [2000]. Briefly, the model uses a semi-Lagrangian approach for the large-scale advection of long-lived species. Vertical mixing of species in the atmospheric boundary layer is modelled following the radiatively driven diurnal variation of the boundary-layer height. Vertical redistribution of chemical species through cloud convection is achieved using a mass-flux cloud scheme. The model uses a comprehensive gas-phase reaction mechanism for NOx, methane, NMHC, biogenic VOCs, and other sulfur and halogen compounds. Specified emissions for anthropogenic

sources is that of EDGAR and GEIA. Geographical distributions of the sinks of important tropospheric species ($O_3$, $NO_2$, PAN, CO, etc) are considered via dry and wet deposition processes. The model uses analyzed winds (1992) from ECMWF, and it contains 19 vertical layers which extends from surface to about 10 hPa. The model horizontal resolution is about 7.5° in longitude and 4.5° in latitude.

## 3. Results

The ozone simulations were performed using the IMS model with analyzed data of zonal wind, meridional wind, temperature, specific humidity, and surface pressure from the European Centre for Medium Range Weather Forecasts (ECMWF) which are updated every 6 hours. The IMS model was multitasked and run parallelly on the shared-memory CRAY J90 [*Wang et al.*, 2000]. The model was run for two years with full tropospheric chemistry, and the results, composed from every 6-hour model output frequency, from the second year were used for the following discussion. We note that the meteorology used here is not directly corresponding to the years where the ozonesonde data were available. Hence, some variability in the distribution of tropospheric ozone can be caused by the interannual variability in the tropics (eg., *Peters et al.*, 2001).

### 3.1. Surface Ozone Distribution

**Figure 1.**

Figure 1 shows modelled surface ozone distributions over most of the marine boundary layer in the Atlantic and the Pacific (from 120°E to 0°W, and from 60°N to 60°S). The model surface ozone in the MBL clearly shows an interhemispheric

asymmetry when compares ozone concentrations at latitudes in the SH to the latitudes in the NH of the Atlantic and the Pacific, respectively. For example, the averaged December ozone concentration over the Atlantic and the Pacific in the NH is higher than in the SH (Figure 1(a)). This northward meridional gradient in ozone concentration in December is reversed to the southward meridional gradient in July (Figure 1(b)), indicating that the model meridional ozone gradients in the MBL always point toward the wintertime hemisphere. The change in the direction of concentration gradients closely follows the seasonal movements.

The model predicts an area of high surface ozone concentrations over the tropical south Atlantic, which extends across southern Africa, the Indian Ocean, and Australia through September to October (Figure 1(c)). Based on satellite and ozonesonde measurements, *Jenkins et al.* [1997] reported that this area shows the highest tropospheric ozone concentrations through September to October. This indicates that the model calculated surface ozone is consistent with the measurements over the southern MBL. Notice that the seasonal tropospheric ozone maximum in the tropical south Atlantic was first recognised from satellite observations by *Fishman et al.* [1986, 1991], followed by many subsequent studies [e.g., *Thompson et al.*, 1996; *Jacob et al.*, 1996; *Diab et al.*, 1996; *Browell et al.*, 1996].

### 3.2. Comparison of Model with Surface Measurements

**Figure 2.**

The results from IMS annual simulations were first compared with surface measurements in the remote MBL environment. Figure 2 shows a global distribution

of the surface and ozonesonde measurement sites used for the following comparison. The annual surface ozone measurements at Westman Is., Bermuda, Mauna Loa, and Samoa were taken from the NOAA CMDL Surface Ozone Data [*S.J. Oltmans*, 2001, personal communications; see also *Oltmans and Levy*, 1994]. In addition to these sites, ozonesonde measurements were taken from the same CMDL source [*S.J. Oltmans*, 2001, personal communications], and the NASA SHADOZ data [*Thompson and Witte*, 1999]. **Figure 3.**

Figure 3 shows time-series plots of modelled and observed $O_3$ levels at four sites located in the remote MBL. We compare model results with two measured $O_3$ levels (for the 1988-1992), one for the daily maximum, and the other one for the daily minimum. While the observed daily minima represent the indigenous local background 'clean' conditions, the observed daily maxima clearly indicate the nonindigenous influences such as elevated $O_3$ from the upper troposphere, or due to the long-range transport of high $O_3$ and anthropogenic $O_3$ precursors from industrial and biomass burning areas. These time-series plots show very distinct and easily identifiable spring ozone maxima at these MBL sites. While it has long been observed that the spring maximum is a NH phenomenon [e.g., *Monks*, 2000], the SH observations at Samoa also shows very distinct spring time maximum comparable to those NH sites.

The observed spring ozone behaviour is generally well reproduced by the model at these sites, and the modelled ozone levels generally fall within the observed ranges at Westman, Bermuda, and Mauna Loa, and is at the upper bound of the observed ozone concentrations at Samoa. Though the model overestimates ozone at some tropical MBL locations, the observed seasonal cycles are closely reproduced by the model. This

indicates that the model is capturing the correct sense of the processes controlling ozone variation at remote MBL environments.

Notice that the time of observed minimum (JJA) is not reproduced by the model at Westman. This indicates that model underestimates the processes contributing to the ozone levels at this location in other seasons. For example, in the simulation without considering tropospheric emissions (see part 3), the model can only produce ozone close to the daily minimum measurements. Hence, the background ozone concentration at higher latitudes is likely to be too low in the seasons through autumn to late winter. The model also overestimates ozone at Samoa, indicating that too much ozone has been transported/produced in the southern MBL.

We note that the observed daily maxima are 2 to 4 times that of the daily minima, indicating that the MBL environment is actually very sensitive to the air from elsewhere such as the upper troposphere and industrial and biomass burning areas. These transport-driven sensitivities are much higher than those driven by the photochemical loss process, which is on the order of no more than a few ppbv per day [e.g., *Paluch et al.*, 1994; *Monks et al.*, 2000]. This indicates that ozone in the MBL at these sites are largely dominated by the processes such as long-range transport of ozone-riched air, cloud convective transport, mixing and dry deposition in the MBL, and cross-tropopause transport.

### 3.3. Comparison of Model with Ozonesondes

While the previous surface comparisons show pronounced seasonal cycles and distinctive interhemispheric asymmetry in $O_3$ in the low latitude MBL, these comparisons were limited to the surface [e.g., *Oltmans et al.*, 1996]. Many components such as free tropospheric $O_3$ and other $O_3$ precursor distribution, $O_3$ exchange in the upper troposphere and lower stratosphere, and atmospheric transport processes are crucial for understanding the chemical behaviour over the remote marine troposphere. In this section we compare modelled ozone vertical profiles with ozonesonde measurements taken from the NASA SHADOZ data and the NOAA CMDL ozone data for the period 1998-1999.

#### 3.3.1. The Atlantic

**Figure 4.**

Figure 4 shows time-height cross sections of measured and modelled $O_3$ at northern (Bermuda) and southern (Ascension Island) Atlantic. For the northern Atlantic site (Figure 4(a)), analyses of one year of vertical soundings of ozone show that high values of ozone extend from the upper troposphere to the middle and lower troposphere during the NH spring (March-May). High levels of ozone are also seen in the lower stratosphere during this period. The model calculated annual variations of ozone in the troposphere at this location is shown in Figure 4(b). The observed high ozone concentrations from the upper to the middle and lower troposphere during the NH spring are generally well reproduced by the model. Both model and ozonesondes show a consistent picture of the ozone distribution in the troposphere during the NH spring compared with other

seasons: Larger ozone concentrations extend downward from the tropopause to near the surface, while smaller ozone concentrations extend upward from the surface to near the tropopause. These characteristics are consistent with other analyses [*Oltmans et al.*, 1996].

*Moody et al.* [1995] suggested that the elevated ozone concentrations in the midtroposphere at this location during this period is associated with downward transport of ozone from the upper and lower stratosphere. Based on the analyses of summer and spring ozonesondes at five locations over the North Atlantic, *Oltmans et al.* [1996] found the connection between large ozone mixing rations and dry air in the middle and upper troposphere with large ozone values in the tropopause region. They suggested that the stratosphere plays a major role in loading the troposphere with ozone, and high ozone events usually extend downward from the tropopause region. From trajectory analyses showing the history of transport path, *Oltmans et al.* [1996] concluded that the upper troposphere and lower stratosphere was the source of elevated ozone in the troposphere.

For the southern Atlantic site (Figure 4(c)), high ozone concentrations are seen in the troposphere during the SH spring (September-November). The spread of high ozone levels extends from the upper troposphere downward to near the surface during this season. Model calculations (Figure 4(d)) at this southern Atlantic site show similar spring ozone maxima extending from the upper troposphere downward, in accordance with the measurements, though the modelled high ozone in the upper troposphere does not extend as far down as in the measurements.

The enhanced tropospheric ozone, which occurs between July and October and observed at Ascension Island, is linked to dry season biomass burning [*Diab et al.*, 1996]. During September-October, gases from extensive fires in Brazil were transported by convective storms into the upper troposphere where tropospheric ozone was photochemically produced and advected eastward over the south Atlantic, while the widespread fires in the deep convection-free central Africa were advected at low altitudes over the Atlantic [*Browell et al.*, 1996; *Jacob et al.*, 1996; *Thompson et al.*, 1996]. The lower modelled ozone concentration in the troposphere compared with the ozonesondes indicate that biomass burning emissions in the equatorial south America and central Africa are too low during the biomass burning season.

The above analyses show an interhemispheric asymmetry in the tropospheric ozone distribution over the Atlantic basin. More persistent and widespread ozone maxima were observed and modelled during the hemispheric spring months, from March to May for the NH, and from September to November for the SH, than any other seasons of the year. Though the season (hemispheric spring) is the same, the sources of elevated ozone in the troposphere are different when comparing the NH with the SH. For the NH Atlantic basin, the downward transport of high ozone from upper troposphere and lower stratosphere are likely to be the major sources. For the SH Atlantic basic, the biomass burning emissions from continents, together with following cloud convective transport and/or large scale transport are likely to be the major contributors (see following part 2 and part 3 papers for further discussions).

### 3.3.2. Western Indian Ocean

**Figure 5.**

Figure 5 shows comparisons of ozone profiles from ozonesondes with model calculations at two locations over the SH western Indian Ocean. Extensive high ozone concentrations from the lower to upper troposphere are seen at these sites. Model calculations show similar SH spring maxima in the troposphere compared with the measurements. Both locations experienced the same sources for the elevated spring ozone in the troposphere as to the SH Atlantic sites of Ascension Island and Natal [*Diab et al.*, 1996; *Baldy et al.*, 1996]. Analysis of one-year ozonesondes at Reunion Island (Figure 5(c)) shows high levels of ozone are observed in the lower to upper troposphere during the SH spring (September-November). *Baldy et al.* [1996] reported that the elevated ozone in the free troposphere during this period of time at this island is concomitant with active biomass burning in the southeastern African continent and Madagascar. *Thompson et al.* [1996] reported that features of elevated tropospheric $O_3$ ($\geq$ 90 ppbv) extend in a band from 0° to 25°S, over SE Indian Ocean, Africa, the Atlantic, and eastern South America during September-October. They showed a strong connection between regions of high ozone and concentrated biomass burning.

### 3.3.3. Western Pacific Ocean

**Figure 6.**

The observations and our previous modelling at sites in the southern Atlantic basin showed that large-scale biomass burning emissions provide sources of elevated ozone over the tropical south Atlantic. Long-range transport of biomass burning pollution could affect ozone on a hemispheric scale [*Fishman et al.*, 1991; *Schultz et al.*, 1999]. Here

we examine the extent of seasonal biomass burning influences over the Pacific basin. Figure 6 show time-height cross sections of vertical ozone profiles form ozonesondes and model calculations at Taiwan (in the subtropical western North Pacific), and Fiji (in the subtropical western South Pacific).

Observed ozone profiles at Taiwan shows similar spring ozone maxima in the troposphere as to the sites in the northern Atlantic, and Hawaii in the eastern North Pacific (see next section). The model shows a similar spring ozone maximum, though the elevated ozone concentrations do not extend as far down to near the surface as in the measurements. The major differences at altitudes below 4 km ($\sim$ 600 hPa) coincide with the altitude range most influenced by continental outflow [e.g., *Kajii et al.*, 1997; *Crawford et al.*, 1997]. This indicates that the model underestimates the impact of continental outflow of $O_3$ precursors such as NO and NMHC [*Crawford et al.*, 1997].

The model calculations at Fiji show that elevated tropospheric ozone occurs in August, and from October onward. The elevated ozone ($\geq$ 40 ppbv) calculated by the model at Java are seen from May to August, instead of measured maxima from October to November. *Schultz et al.* [1999] reported the importance of biomass burning emissions in South America and Africa for the ozone budget at higher altitudes, and the NOx decomposed from transported PAN at altitudes below 4 km over the tropical South Pacific. This indicates that the model underestimates the impact from biomass burning emissions and the long-range transport of reactive nitrogen at Java, while overestimating the impact of biomass burning emissions at Fiji.

### 3.3.5. Central to Eastern Pacific

**Figure 7.**

The South Pacific is the region of the tropical troposphere most remote from human activity [*Schultz et al.*, 1999]. Figure 7 (c) shows ozone vertical profiles from ozonesondes at Tahiti. At this location, an identifiable SH spring ozone maxima are seen as elevated ozone concentrations extend from upper troposphere downward to the middle troposphere. The timing of this ozone maxima, from September to November, coinciding with the intensive SH biomass burning activities take place in South America, Africa, Southeast Asia, and Oceania [*Schultz et al.*, 1999]. Elevated ozone ($\geq$ 40 ppbv) levels extend from the upper to the middle troposphere at Samoa in October.

The measurements also exhibit another period of elevated ozone ($\geq$ 40 ppbv) in the upper troposphere in June-July. The model calculations show that elevated ozone extends from the upper to the middle troposphere at this period, indicating the contribution of biomass burning emissions. However, the model does not show the elevated ozone as observed in September-October. Modelled ozone vertical profiles at South Pacific sites (Java, Fiji, Samoa, and Tahiti) are persistently higher than the observations in June-July, indicating that the model contains too much local biomass burning emissions, or too much biomass burning is transported into this area from Africa or South America. On the other hand, less biomass burning emissions has been produced or transported into South Pacific during September-October.

For the NH site of Hawaii, both observed and modelled ozone profiles show very distinctive seasonal spring maximum. Elevated ozone levels extend from upper

troposphere to near the surface. Seasonal minima appear during the summer months. *Wang et al.* [1998] attributed this strong spring maximum to the long-range transport of Asian pollution over the North Pacific. Analyses of anthropogenic aerosols [*Perry et al.*, 1999] and CO [*Jaffe et al.*, 1997] at this site also shows a seasonal maximum in spring with sources from Asia continent [*Perry et al.*, 1999].

In summary, the comparison of time series ozone vertical distribution at Pacific basin shows an interhemispheric asymmetry in ozone concentrations between NH and SH subtropics. While the NH spring maxima are maintained by the continental outflow and long-range transport of continental anthropogenic pollutants, the SH spring maxima are likely due to the biomass burning emissions which take place in Southeast Asia, Oceania, southern Africa, and South America, and transport of $O_3$ precursors such as PAN and NOx from soil and lightning [*Schultz et al.*, 1999].

### 3.3.6. Northern Higher Latitudes

**Figure 8.**

Figure 8 extends the comparison of ozone vertical distribution from ozonesonde measurements with model to higher latitude locations in the NH. Both model and measurements at Trinidadhead and Boulder show highest ozone in spring in the lower stratosphere (200 hPa), and in April to August in the middle troposphere and near the surface. Limited ozonesonde measurements and model calculations at Fairbanks show similar timing for the occurrence of spring ozone maximum compared with Trinidadhead and Boulder. Model calculations at the Azores show elevated ozone in the lower stratosphere in spring, in the middle troposphere in spring to summer, and in spring in

the lower troposphere. These characteristics, high ozone extending downward from the tropopause region, are close to the available measurements [*Oltmans et al.*, 1996].

## 4. Summary

In this papers we present modelling results from a 3D CTM for the global troposphere. The modelled results are examined at the surface and on a series of time-height cross sections at several locations spread over the Atlantic, the Indian, and the Pacific. Comparison of model with surface measurements at remote MBL stations indicate a close agreement. The most striking feature of the hemispheric spring ozone maximum in the MBL can be most easily identified from these NOAA CMDL surface ozone measurements, at the NH sites of Westman Island, Bermuda, and Mauna Loa, and at the SH site of Samoa. Modelled ozone vertical distribution in the troposphere are compared with ozone profiles from NOAA CMDL and NASA SHADOZ ozonesonde measurements. For the Atlantic and the Indian sites, the model generally produces a hemispheric spring ozone maximum close to those of the measurements. The model also produces the spring ozone maximum in the northeastern and tropical north Pacific close to those measurements, and at sites in the NH high latitudes. The close agreement between model and the measurements indicate that the model can reproduce the proposed processes responsible for producing the spring ozone maximum in these regions of the MBL, lending confidence in the use of the model to investigate MBL ozone chemistry. Overall, the model appears to perform better at sites where stratospheric and biomass burning emissions is the major contributor. For example, for

sites at the Atlantic basin, western Indian (except Nairobi), central north Pacific, and the NH high latitudes. The model performance is degraded as the distance between the site and the continental source increase, or as the site located close to the equator (e.g., San Cristobal and Nairobi), where the complex tropical circulations (e.g., Walker circulations and Hadley circulations) and deep cloud convections are more difficult for a model to handle well. Other factors such as dry deposition, heterogeneous chemistry, halogen chemistry, model resolution, and cross tropopause transport can all affect model results and need further investigations. In the following two papers (Parts 2 and 3) we investigate the impact of stratosphere-troposphere exchange and biomass burning emission on the simulated ozone distribution, respectively.

**Acknowledgments.** The authors like to thank BADC, ECMWF, Central Weather Bureau (Taiwan), S.J. Oltmans, W.-S. Kau, G. Carver, and Brian Doty for their support on this work. We are very grateful to the NASA SHADOZ project for the ozonesonde data archive (http://hyperion.gsfc.nasa.gov/Dataservices/shadoz/Sites2.html). This research was supported by the NSC grant NSC-89-2119-M-008-007. The Centre for Atmospheric Science is a joint initiative of the Department of Chemistry and the Department of Applied Mathematics and Theoretical Physics. This work forms part of the NERC U.K. Universities Global Atmospheric Modeling Programme.

## References


Ariya, P.A., Jobson, B.T., Sander, R., Niki, H., Harris, G.W., Hopper, J.F., Anlauf, K.G., 1998. Measurements of $C_2$-$C_7$ hydrocarbons during the Polar Sunrise Experiment 1994: Further evidence for halogen chemistry in the troposphere, *Journal of Geophysical Research*, **103**, 13,169–13,180.

Baldy, S., Ancellet, G., Bessafi, M., Badr, A., Lan Sun Luk, D., 1996. Field observations of the vertical distribution of tropospheric ozone at the island of Reunion (southern tropics), *Journal of Geophysical Research*, **101**, 23,835–23,849, 1996.

Board, A.S., Fuelberg, H.E., Gregory, G.L., Heikes, B.G., Schultz, M.G., Blake, D.R., Dibb, J.E., Sandholm, S.T., Talbot, R.W., 1999. Chemical characteristics of air from differing source regions during the Pacific Exploratory Mission-Tropics A (PEM-Tropics A), *Journal of Geophysical Research*, **104**, 16,181–16,196.

Browell, E.V., Fenn, M.A., Butler, C.F., Grant, W.B., Clayton, M.B., Fishman, J., Bachmeier, A.S., Anderson, B.E., Gregory, G.L., Fuelberg, H.E., Bradshaw, D., Sandholm, S.T., Blake, D.R., Heikes, B.G., Sachse, G.W., Singh, H.B., Talbot, R.W., 1996. Ozone and aerosol distributions and air mass characteristics over the South Atlantic Basin during the burning season, *Journal of Geophysical Research*, **101**, 24,043–24,068.

Crawford, J., Davis, D., Chen, G., Bradshaw, J., Sandholm, S., Kondo, Y., Liu, S., Browell, E., Gregory, G., Anderson, B., Sachse, G., Collins, J., Barrick, J., Blake, D., Talbot, R., Singh, H., 1997. As assessment of ozone photochemistry in the extratropical western North Pacific: Impact of continental outflow during the late winter/early spring, *Journal of Geophysical Research*, **102**, No. D23, 28,469–28,487.

Diab, R.D., Thompson, A.M., Zunckel, M., Coetzee, G.J.R., Combrink, J., Bodeker, G.E., Fishman, J., Sokolic, F., McNamara, D.P., Archer, C.B., Nganga, D., 1996. Vertical ozone distribution over southern Africa and adjacent oceans during SAFARI-92, *Journal of Geophysical Research*, **101**, No. D19, 23,823–23,833.

Dickerson, R.R., Rhoads, K.P., Carsey, T.P., Oltmans, S.J., Burrows, J.P., Crutzen, P.J., 1999. Ozone in the remote marine boundary layer: A possible role for halogens, *Journal of Geophysical Research*, **104**, 21,385–21,395.

Finnan, J.M., Jones, M.B., Burke, J.I., 1996. A time-concentration study on the effects of ozone on spring wheat (Triticum aestivum L.) 1. Effects on yield, *Agriculture Ecosystems and Environment*, **57**, 159–167.

Fishman, J., Minnis, P., Reichle Jr., H.G., 1986. The use of satellite data to study tropospheric ozone in the tropics, *Journal of Geophysical Research*, **91**, 14,451–14,465.

Fishman, J., Fakhruzzaman, K., Cros, B., Nganga, D., 1991. Identification of widespread pollution in the Southern Hemisphere deduced from satellite analyses, *Science*, **252**, 1693–1696.

Jacob, D.J., Heikes, B.G., Fan, S.-M., Logan, J.A., Mauzerall, D.L., Bradshaw, J.D., Singh, H.B., Gregory, G.L., Talbot, R.W., Blake, D.R., Sachse, G.W., 1996. Origin of ozone and NOx in the tropical troposphere: A photochemical analysis of aircraft observations over the South Atlantic basic, *Journal of Geophysical Research*, **101**, 24,235–24,250.

Jaffe, D.A., Hornrath, R.E., Zhang, L., Akimoto, H., Shimizu, A., Mukai, H., Murano, K., Hatakeyama, S., Merrill, J., 1996. Measurements of NO, NOy, CO, and $O_3$ and estimation of the ozone production rate at Oki Island, Japan, during PEM-West, *Journal of Geophysical Research*, **101**, 2037–2048.

Jaffe, D., Mahura, A., Kelly, J., Atkins, J., Novelli, P.C., Merrill, J., 1997. Impact of Asian emissions on the remote North Pacific atmosphere: Interpretation of CO data from Shemya, Guam, Midway and Mauna Loa, *Journal of Geophysical Research*, **102**, 28,627–28,635.

Jenkins, G.S., Mohr, K., Morris, V.R., Arino, O., 1997. The role of convective processes over the Zaire-Congo basin to the southern hemispheric ozone maximum, *Journal of Geophysical Research*, **102**, 18,963–18,980, 1997.

Johnson, J.E., Gammon, R.H., Larsen, J., Bates, T.S., Oltmans, S.J., Farmer, J.C., 1990. Ozone in the marine boundary layer over the Pacific and Indian Oceans: Latitudinal gradients and diurnal cycles, *Journal of Geophysical Research*, **95**, 11,847-11,856.

Junkermann, W., Stockwell, W.R., 1999. On the budget of photooxidants in the marine boundary layer of the tropical South Atlantic, *Journal of Geophysical Research*, **104**, 8039–8046.

Kajii, Y., Akimoto, H., Komazaki, Y., Tanaka, S., Mukai, H., Murano, K., Merrill, J.T., 1997. Long-range transport of ozone, carbon monoxide, and acidic trace gases at Oki Island, Japan, during PEM-West B / PEACAMPOT B campaign, *Journal of Geophysical Research*, **102**, 28,637–28,649.

Kawa, S.R., Pearson Jr., R., 1989. Ozone budgets from the dynamics and chemistry of marine stratocumulus experiment, *Journal of Geophysical Research*, **94**, No. D7, 9809–9817.

Kley, D., Crutzen, P.J., Smit, H.G.J., Vömel, H., Oltmans, S.J., Grassl, H., Ramanathan, V., 1996. Observations of near-zero ozone concentrations over the convective Pacific: Effects on air chemistry, *Science*, **274**, 230–233.

Künzli, N., Kaiser, R., Medina, S., Studnicka, M., Chanel, O., Filliger, P., Herry, M., Horak, F., Puybonnieux-Texier, V., Quénel, P., Schneider, J., Seethaler, R., Vergnaud, J.-C., Sommer, H., 2000. Public-health impact of outdoor and traffic-related air polution: a European assessment, *Lancet*, **356**, 795–801.

Lal, S., Naja, M., Jayarama, A., 1998. Ozone in the marine boundary layer over the tropical Indian Ocean, *Journal of Geophysical Research*, **103**, 18,907–18,917.

Latt, A.T.J., Zachariasse, M., Roelofs, G.J., van Velthoven, P., Dickerson, R.R., Rhoads, K.P., Oltmans, S.J., Lelieveld, J., 1995. Tropospheric $O_3$ distribution over the Indian Ocean during spring 1995 evaluated with a chemistry-climate model, *Journal of Geophysical Research*, **104**, 13,881–13,893.

Logan, J.A., 1999a. An analysis of ozonesonde data for the troposphere: Recommendations for testing 3-D models and development of a gridded climatology for tropospheric ozone, *Journal of Geophysical Research*, **104**, 16,115–16,149.

Logan, J.A., 1999b. An analysis of ozonesonde data for the lower stratosphere: Recommendations for testing models, *Journal of Geophysical Research*, **104**, 16,151–16,170.

Monks, P.S., Sailsbury, G., Holland, G., Penkett, S.A., Ayers, G.P., 2000. A seasonal comparison of ozone photochemistry in the remote marine boundary layer, *Atmospheric Environment*, **34**, 2547–2561.

Monks, P.S., 2000. A review of the observations and origins of the spring ozone maximum, *Atmospheric Environment*, **34**, 3545–3561.

Moody, J.L., Oltmans, S.L., Levy II, H., Merrill, J.T., 1995. Transport climatology of tropospheric ozone: Bermuda, 1988-1991, *Journal of Geophysical Research*, **100**, 7179–7194.

Müller, J.-F., Brasseur, G., 1995. IMAGES: A Three-Dimensional Chemical Transport Model of the Global Troposphere, *Journal of Geophysical Research*, **100**, 16445-16490.

Murphy, D.M., Fahey, D.W., 1994. An estimate of the flux of stratospheric reactive nitrogen and ozone into the troposphere, *Journal of Geophysical Research*, **99**, 5325–5332.

Nagao, I., Matsumoto, K., Tanaka, H., 1999. Sunrise ozone destruction in the sub-tropical marine boundary layer, *Geophysical Research Letters*, **26**, 3377–3380.

Oltmans, S.J., Levy II, H., Merrill, J.M., Moody, J.L., Lathrop, J.A., Cuevas, E., Trainer, M., O'Neill, M.S., Prospero, J.M., Vömel, H., Johnson, B.J., 1996. Summer and spring ozone profiles over the Atlantic from ozonesonde measurements, *Journal of Geophysical Research*, **101**, 29,179–29,200.

Oltmans, S.J., Levy II, H., 1994. Surface ozone measurements from a global network, *Atmospheric Environment*, **28**, 9–24.

Paluch, I.R., Lenschow, D.H., Siems, S., McKeen, S., Kok, G.L., Schillaski, R.D., 1994. Evolution of the subtropical marine boundary layer: Comparison of soundings over the eastern Pacific from FIRE and HaRP, *Journal of the Atmospheric Sciences*, **51**, 1465–1479.

Penkett, S.A., Reeves, C.E., Bandy, B.J., Kent, J.M., Richer, H.R., 1998. Comparison of calculated and measured peroxide data collected in marine air to investigate prominent features of the annual cycle of ozone in the troposphere, *Journal of Geophysical Research*, **103**, 13,377–13,388.

Perry, K.D., Cahill, T.A., Schnell, R.C., Harris, J.M., 1999., Long-range transport of anthropogenic aerosols to the National Oceanic and Atmospheric Administration baseline station at Mauna Loa Observatory, Hawaii, *Journal of Geophysical Research*, **104**, 18,521–18,533.

Peters, W., Krol, M., Dentener, F., Lelieveld, J., 2001., Identification of an El Nino-Southern Oscillation signal in a multiyear global simulation of tropospheric ozone, *Journal of Geophysical Research*, **106**, 10,389–10,402.

Piotrowicz, S., Boran, D.A., Fischer, C.J., 1986. Ozone in the boundary layer of the equatorial Pacific Ocean, *Journal of Geophysical Research*, **91**, 13,113–13,119.

Piotrowicz, S.R., Bezdek, H.F., Harvey, G.R., Springer-Young, M., 1991. On the ozone minimum over the equatorial Pacific Ocean, *Journal of Geophysical Research*, **96**, 18,679–18,687.

Pochanart, P., Hirokawa, J., Kajii, Y., Akimoto, H., Nakao, M., 1999. Influence of regional-scale anthropogenic activity in northeast Asia on seasonal variations of surface ozone and carbon monoxide observed at Oki, Japan, *Journal of Geophysical Research*, **104**, 3621–3631.

Roelofs, G.-J., Lelieveld, J., 1997. Model study of the influence of cross-tropopause $O_3$ transport on the tropospheric $O_3$ levels, *Tellus*, **49B**, 38–55.

Roelofs, G.-J., Lelieveld, J., von Dorland, R., 1997. A three-dimensional chemistry/general circulation model simulation of anthropogenically derived ozone in the troposphere and its radiative climate forcing, *Journal of Geophysical Research*, **102**, 23,389–23,401.

Schultz, M.G., Jacob, D.J., Wang, Y., Logan, J.A., Atlas, E.L., Blake, D.R., Blake, N.J., Bradshaw, J.D., Browell, E.V., Fenn, M.A., Flocke, F., Gregory, G.L., Heikes, B.G., Sachse, G.W., Sandholm, S.T., Shetter, R.E., Singh, H.B., Talbot, R.W., 1999. On the origin of tropospheric ozone and NOx over the tropical South Pacific, *Journal of Geophysical Research*, **104**, 5829–5843.

Singh, H.B. Gregory, G.L., Anderson, A., Browell, E., Sachse, G.W., Davis, D.D., Crawford, J., Bradshaw, J.D., Talbot, R., Blake, D.R., Thornton, D., Newell, R., Merrill, J., 1996. Low ozone in the marine boundary layer of the tropical Pacific Ocean: Photochemical loss, chlorine atoms, and entrainment, *Journal of Geophysical Research*, **101**, 1907–1917.

Thompson, A.M., Pickering, K.E., McNamara, D.P., Schoeberl, M.R., Hudson, R.D., Kim, J.H., Browell, E.V., Kirchhoff, V.W.J.H., Nganga, D., 1996. Where did tropospheric ozone over southern Africa and the tropical Atlantic come from in October 1992? Insights from TOMS, GTE TRACE A, and SAFARI 1992, *Journal of Geophysical Research*, **101**, 24,251–24,278.

Thompson, A.M., Witte, J.C., 1999. A new data set for the earth science community, *Earth Observer*, **11**, 27–30.

Wang, K.-Y., Pyle, J.A., Sanderson, M.G., Bridgeman, C., 1999. Implementation of a convective atmospheric boundary layer scheme in a tropospheric chemistry transport model, *Journal of Geophysical Research*, **104**, 23,729–23,745.

Wang, K.-Y., Shallcross, D.E., 2000. A Lagrangian study of the three-dimensional transport of boundary-layer tracers in an idealised baroclinic-wave life-cycle, *Journal of Atmospheric Chemistry*, **35**, 227–247.

Wang, K.-Y., Lary, D.J., Hall, S.M., 2000. Improvement of a 3-D CTM and a 4-D variational data assimilation on a vector machine CRAY J90 through a multitasking strategy, *Computer Physics Communications*, **125**, 142–153.

Wang, K.-Y., Pyle, J.A., Shallcross, D.E., 2001a. Formulation and evaluation of IMS, an interactive three-dimensional tropospheric chemical transport model 1. Model emission schemes and transport processes, *Journal of Atmospheric Chemistry*, **38**, 195–227.

Wang, K.-Y., Pyle, J.A., Shallcross, D.E., Lary, D.J., 2001b. Formulation and evaluation of IMS, an interactive three-dimensional tropospheric chemical transport model 2. Model chemistry and comparison of modelled $CH_4$, CO, and $O_3$ with surface measurements, *Journal of Atmospheric Chemistry*, **38**, 31–71.

Wang, Y., Logan, J.A., Jacob, D.J., 1998. Global simulation of tropospheric $O_3$-$NO_x$-hydrocarbon chemistry 3. Origin of tropospheric ozone and effects of nomenthane hydrocarbons, *Journal of Geophysical Research*, **103**, 10,757–10,767.

Winkler, P., 1988. Surface ozone over the Atlantic Ocean, *Journal of Atmospheric Chemistry*, **7**, 73–91.

Yienger, J.J., Klonecki, A.A., Levy II, H., Moxim, W.J., Carmichael, G.R., 1999. An evaluation of chemistry's role in the winter-spring ozone maximum found in the northern midlatitude free troposphere, *Journal of Geophysical Research*, **104**, 3655–3667.

---

K.-Y. Wang, Centre for Atmospheric Science, Department of Chemistry, Cambridge University, Lensfield Road, Cambridge, CB2 1EW, U.K.

D.E. Shallcross, School of Chemistry, University of Bristol, BS8 1TS, U.K.

J.A. Pyle, Centre for Atmospheric Science, Department of Chemistry, Cambridge University, Lensfield Road, Cambridge, CB2 1EW, U.K.

Received _____

---

This manuscript was prepared with AGU's LaTeX macros v5, with the extension package 'AGU$^{++}$' by P. W. Daly, version 1.6b from 1999/08/19.

## Figure Captions

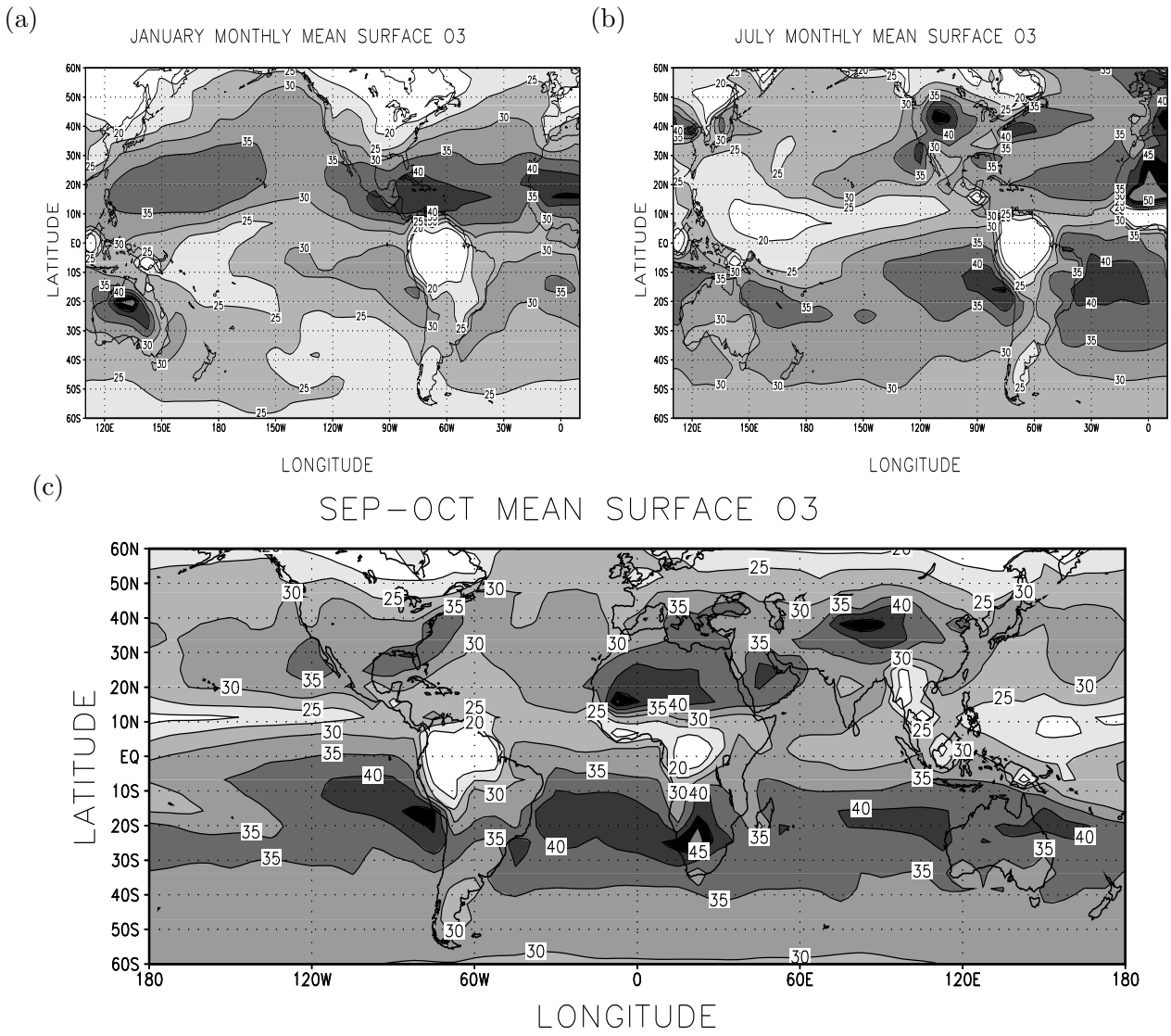


**Figure 1.** Monthly mean ozone distributions (ppbv) calculated at the surface for (a) January, (b) July, and (c) September to October.

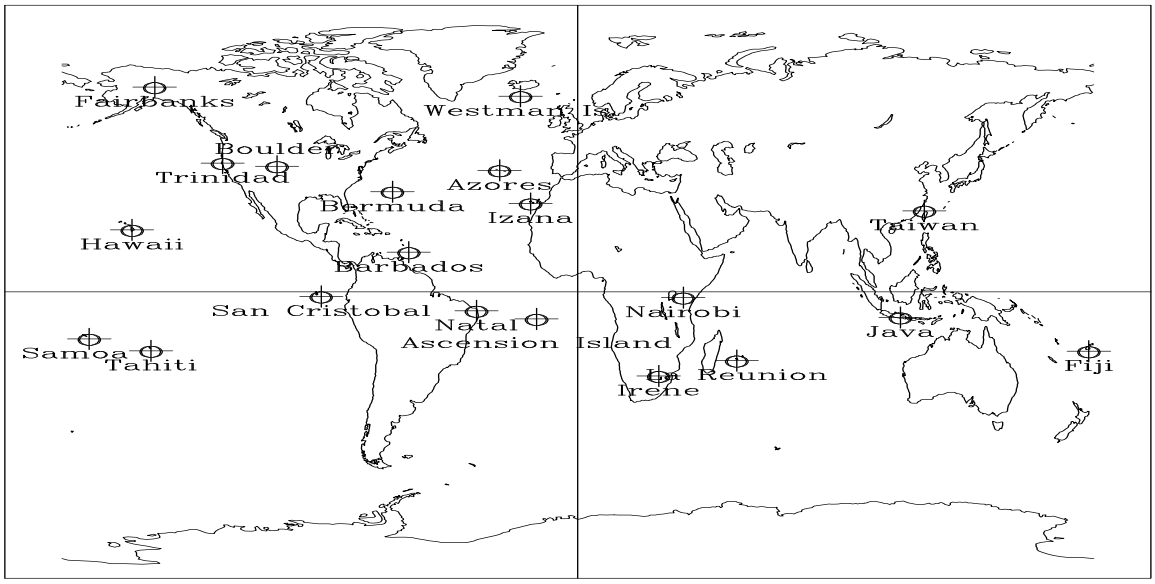


**Figure 2.** Distribution of surface and ozonesonde measurement sites used for this study.

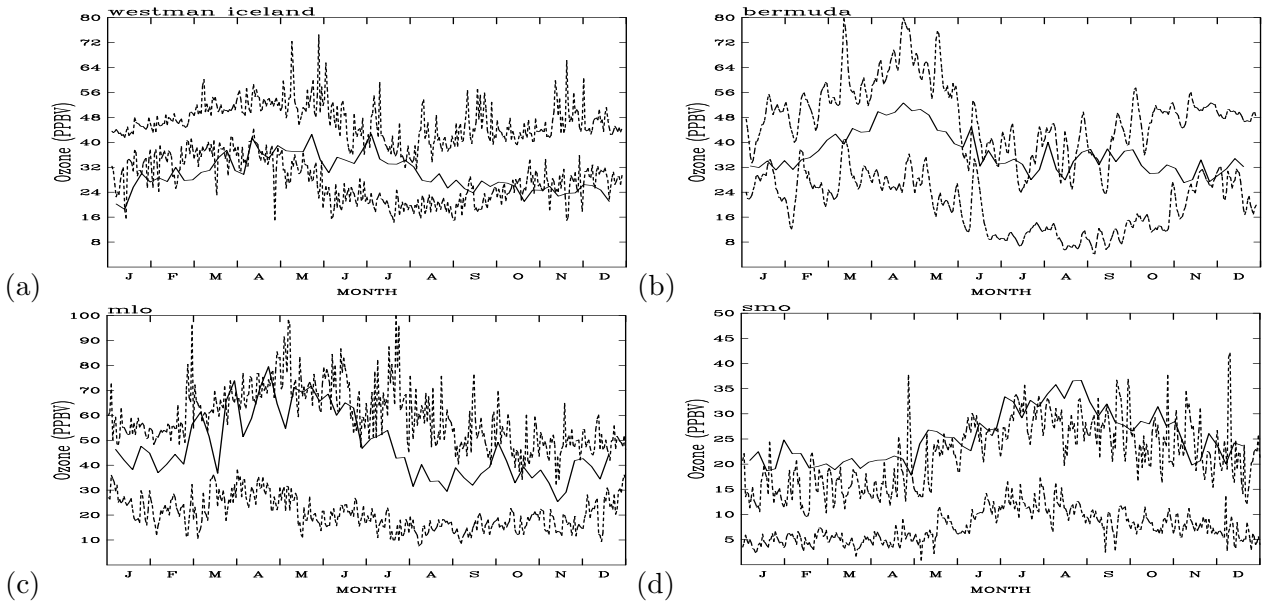


**Figure 3.** Comparison of modelled (solid thick lines) seasonal cycles of $O_3$ (ppbv) at (a) Westman, Iceland, (b) Bermuda, (c) Mauna Loa, and (d) Samoa with the measurements (thin dashed lines). Two measured $O_3$ levels (for 1988-1992, except at Westman where the 1992-1997 data were used) are shown here, one for the daily maximum, while the other one for the daily minimum.

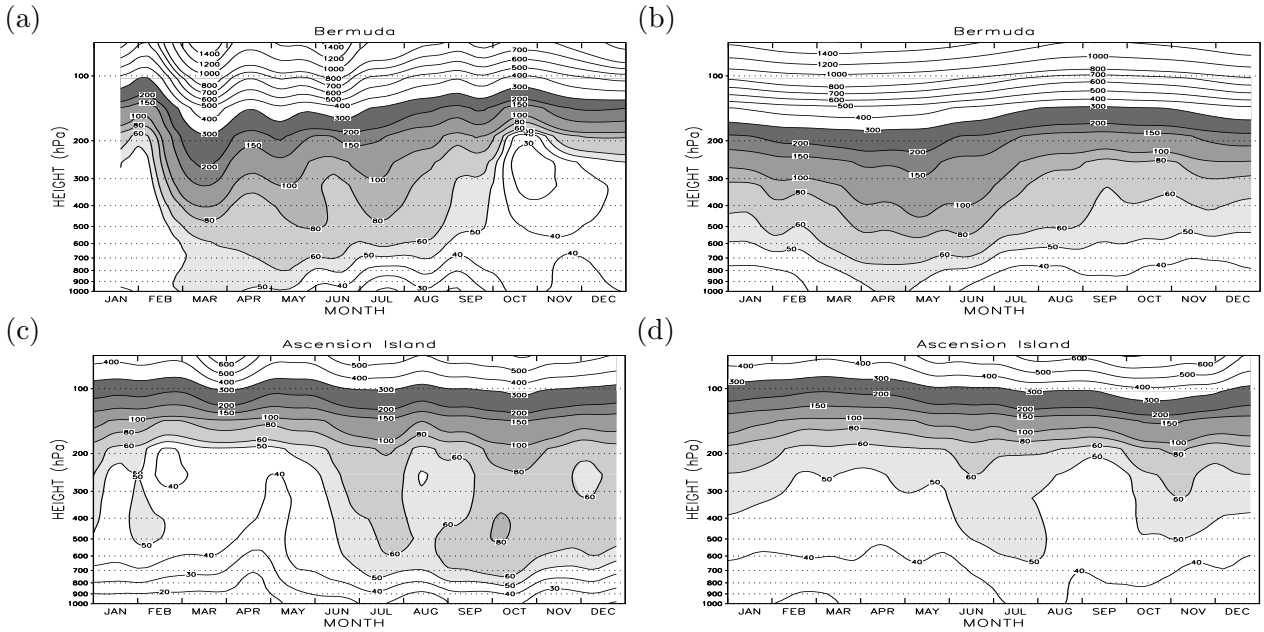


**Figure 4.** Time-height cross sections of $O_3$ (ppbv) from measurements at Bermuda (32°N, 65∘W) (a) and Ascension Island (8°S, 14°W) (c). The model calculation for these locations are shown in (b) and (d), respectively.

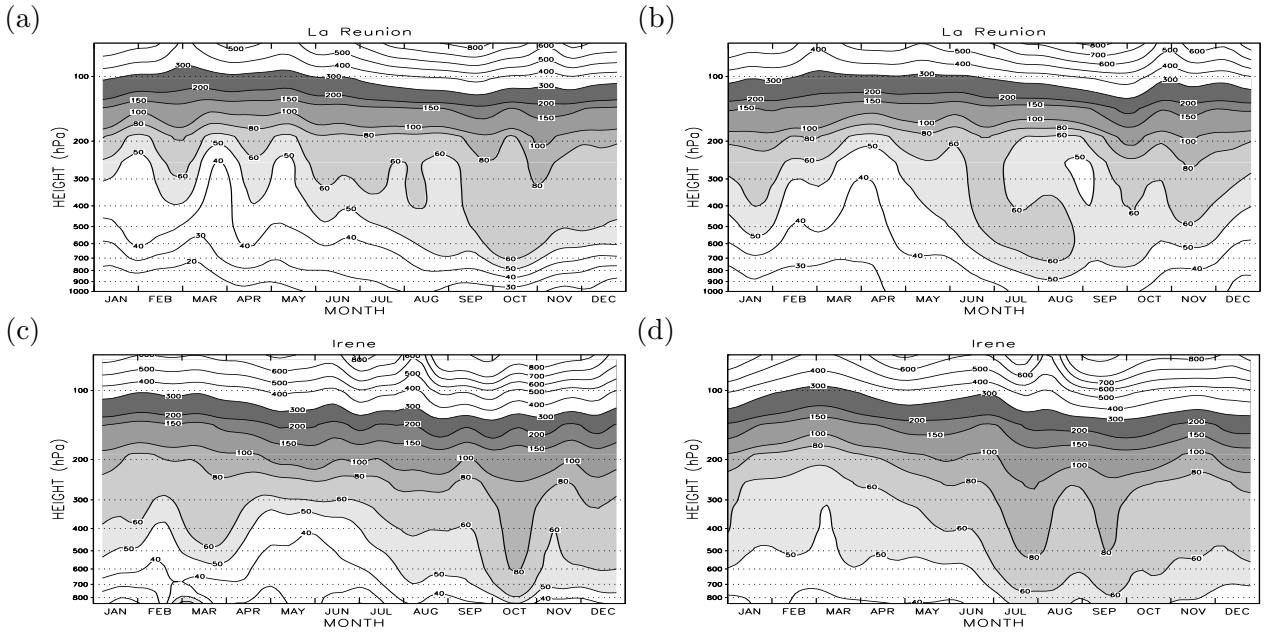


**Figure 5.** Time-height cross sections of $O_3$ (ppbv) from measurements at La Reunion (21°S, 56°E) (a) and Irene (26°S, 28°E) (c). The model calculation for these locations are shown in (b) and (d), respectively.

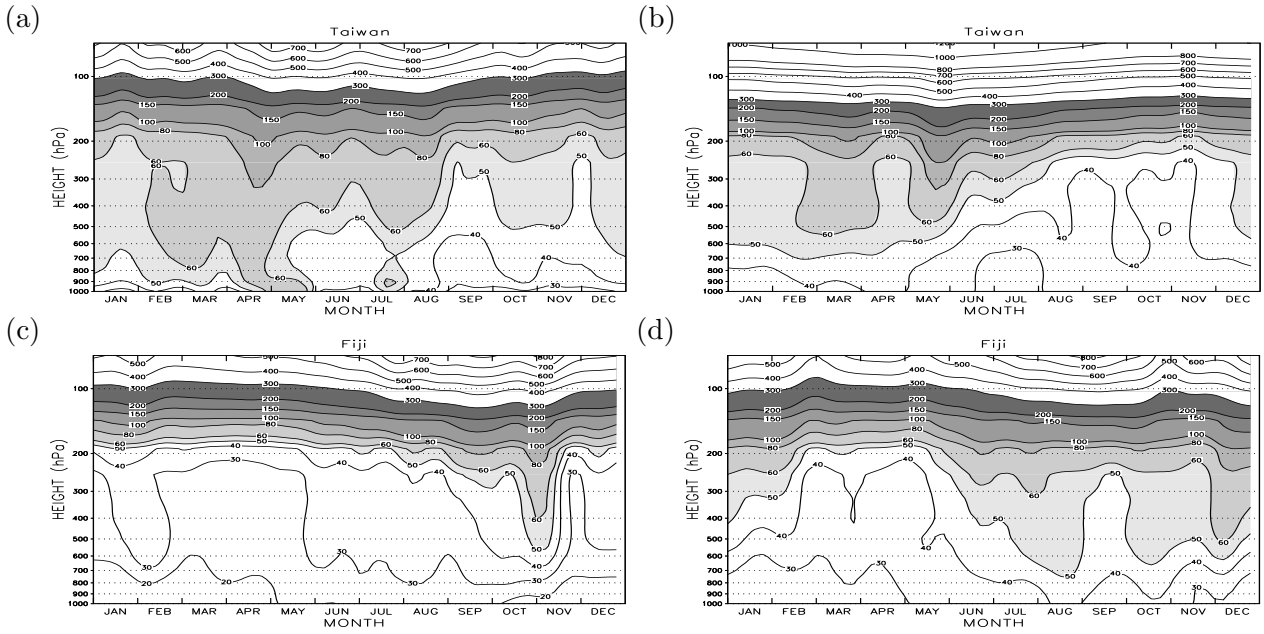


**Figure 6.** Time-height cross sections of $O_3$ (ppbv) from measurements at Taiwan (25°N, 121°E) (a) and Fiji (17°S, 179°E) (c). The model calculation for these locations are shown in (b) and (d), respectively.

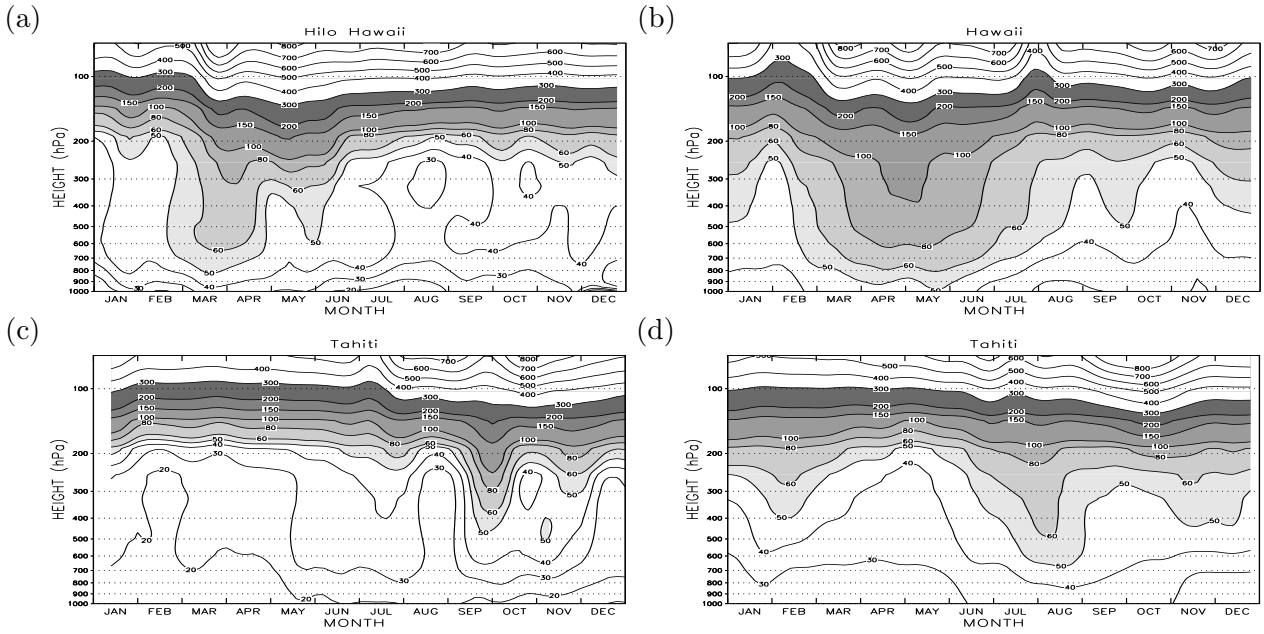


**Figure 7.** Time-height cross sections of $O_3$ (ppbv) from measurements at Hawaii (20°N, 155°W) (a) and Tahiti (18°S, 149°W) (c). The model calculation for these locations are shown in (b) and (d), respectively.

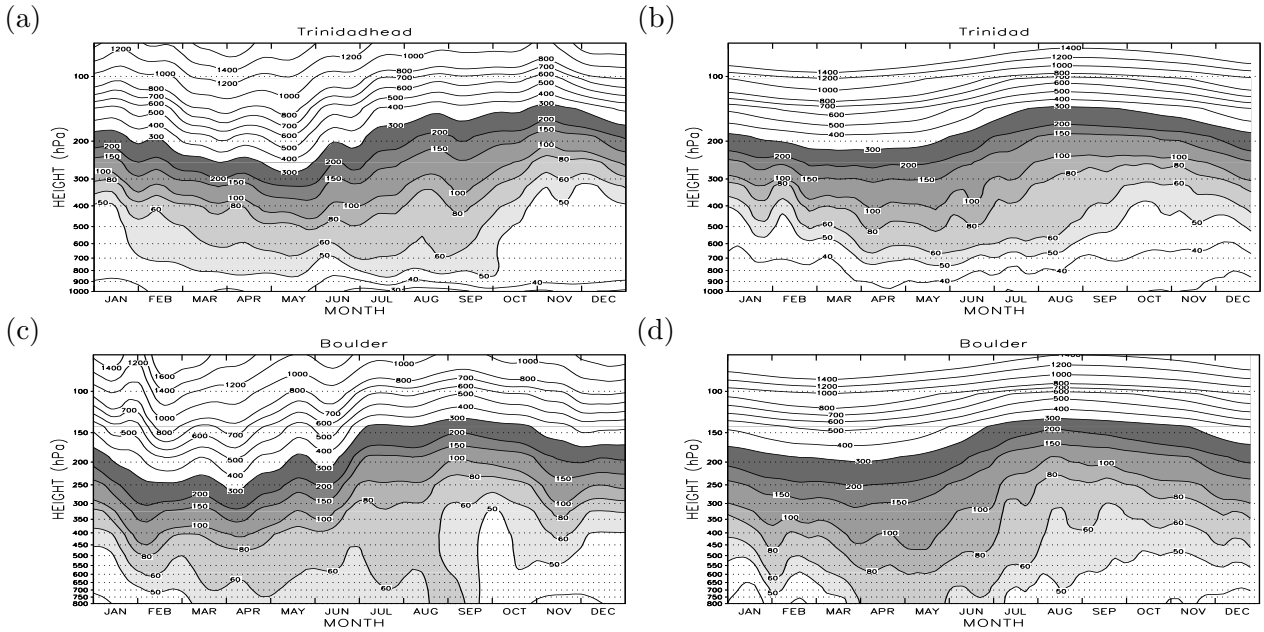


**Figure 8.** Time-height cross sections of $O_3$ (ppbv) from measurements at Trinidadhead (41°N, 124°W) (a) and Boulder (40°N, 105°W) (c). The model calculation for these locations are shown in (b) and (d), respectively.